ANZIAM J. **64** (2022), 292–313
doi:10.1017/S1446181123000020

A MODIFICATION TO THE SCHRÖDINGER EQUATION FOR BROADER BANDWIDTH GRAVITY-CAPILLARY WAVES ON DEEP WATER WITH DEPTH-UNIFORM CURRENT

SOURAV HALDER[1] and ASOKE KUMAR DHAR[1]

(Received 30 March, 2022; accepted 21 January, 2023; first published online 3 March, 2023)

Abstract

We derive a nonlinear Schrödinger equation for the propagation of the three-dimensional broader bandwidth gravity-capillary waves including the effect of depth-uniform current. In this derivation, the restriction of narrow bandwidth constraint is extended, so that this equation will be more appropriate for application to a realistic sea wave spectrum. From this equation, an instability condition is obtained and then instability regions in the perturbed wavenumber space for a uniform wave train are drawn, which are in good agreement with the exact numerical results. As it turns out, the corrections to the stability properties that occur at the fourth-order term arise from an interaction between the mean flow and the frequency-dispersion term. Since the frequency-dispersion term, in the absence of depth-uniform current, for pure capillary waves is of opposite sign for pure gravity waves, so too are the corrections to the instability properties.

2020 *Mathematics subject classification*: primary 76B07; secondary 76B15, 76B45.

Keywords and phrases: nonlinear Schrödinger equation, gravity-capillary waves, depth-uniform current, broader bandwidth, modulational instability.

1. Introduction

The nonlinear wave–current interactions attract the attention of researchers in ocean engineering owing to the almost always co-existence of waves with current. It is a well-known fact that currents can significantly alter the characteristics of surface waves [3, 15, 19]. From some preceding studies, it has been established that the interactions between waves and currents essentially depend on the propagation direction of waves and the depth-uniform current. Research on wave–current interactions have often

[1]Department of Mathematics, Indian Institute of Engineering Science and Technology, Shibpur, Howrah 711103, West Bengal, India; e-mail: souravhalder76@gmail.com, asoke.dhar@gmail.com

supposed that current is uniform with depth [13, 25, 28, 27]. Thus, it is necessary to derive an equation which deals with the effect of depth-uniform current. In the analysis of nonlinear evolution of water waves, the nonlinear Schrödinger equation (NLSE) is frequently used as it can appropriately reflect the modulational instability. A cubic NLSE including the effects of slowly varying depth and current on the evolution of Stokes wavepacket was investigated by Turpin et al. [30]. The numerical result shows that the nonlinear evolution of a wavepacket is directly related to the instability parameter, which depends strongly on the current and depth variation. A following current has a stabilizing effect on a wave train, whereas a reverse current can cause major wave train changes in all depths. Gerber [11] investigated a cubic NLSE for surface waves on deep water in the presence of a current, and specified that for the waves propagating in the same direction as the current, the current had a stabilizing effect on the waves. Further, for an adverse current gradient, a rapid destabilization of the waves was predicted. This is due to the steepening effect of the current, as well as the shorter time required for an equivalent amount of growth of the sidebands, when compared with the still-water case. Stocker and Peregrine [25] made an extension of Dysthe's [10] work to cover the effect of depth-uniform current. Later, Onorato et al. [22] used the current-modified NLSE of Hjelmervik and Trulsen [13] to investigate the effect of currents on the modulational instability, and argued that an initially stable wave train in still water would become unstable after entering an adverse depth-uniform current region.

In general, gravity-capillary waves are formed by wind and generate a fluid flow in the topmost water layer. In the incipient evolution of wind waves, these waves play an important role in contributing, to some extent, to the ocean surface stress and consequently participate in air–ocean momentum transfer. Accurate representation of the stress is useful in modelling and predicting ocean wave dynamics. Debsarma and Das [6] derived a fourth-order nonlinear evolution equation (NLEE) for gravity-capillary waves with a thin thermocline in infinite depth of water, and based on this equation, they made a stability analysis of a uniform wave train. Brantenberg and Brevik [2] used a third-order Stokes expansion for periodic gravity-capillary waves moving on an opposing current. The stability of gravity-capillary waves for irrotational motion was studied by several authors such as Hogan [14], Djordjevic and Redekopp [9] based on fourth- and third-order envelope equations, respectively. Moreover, Chen and Saffman [5], Tiron and Choi [26] made the numerical computations extended to capillary waves, and Zhang and Melville [33] investigated the stability of gravity-capillary waves numerically including three-wave and five-wave resonant interactions, apart from four-wave interaction.

The nonlinear spatio-temporal evolution of weak nonlinear surface waves can be analysed by the cubic NLSE if the wave steepness is small, so that $ka \ll 1$ and the wave bandwidth is narrow ($|\Delta \boldsymbol{k}|/k \ll 1$), where $k, a, \Delta \boldsymbol{k}$ stand for the characteristic wavenumber, amplitude and modulation wave vector, respectively. Here, one assumes that the wave steepness and the bandwidth are of an identical order of magnitude $O(\epsilon)$, for which the governing nonlinear and dispersive effects balance at third-order $O(\epsilon^3)$.

https://doi.org/10.1017/S1446181123000020 Published online by Cambridge University Press

The resulting third-order NLSE for gravity-capillary waves were derived by Kawahara [16], and Djordjevic and Redekopp [9] on finite depth. Dysthe [10] derived an evolution equation for surface gravity waves on deep water by extending the perturbation analysis one step further which included the fourth-order terms in the cubic NLSE, and Brinch-Nielsen and Jonsson [4] derived fourth-order NLSE on arbitrary depth of water. Later, Dhar and Das [7] made an extension of Dysthe's [10] work in the presence of air flowing over water. Although the stability analysis made from fourth-order NLSE gives excellent results compared to the third-order equation, the limitation in wave bandwidth severely restricts the applicability of third- and fourth-order Schrödinger equations for three-dimensional sea waves in two ways. First, the ocean wave spectra from the continental shelf are often bandwidth restricted, but have bandwidths exceeding the above restriction. Second, these evolution equations have instability regions for a finite amplitude wave extending outside the narrow bandwidth constraint. To avoid the restriction in bandwidth, Zakharov's integral equation [24, 32] has been modelled. Notwithstanding the Zakharov equation being more general, it is more costly to evaluate numerically compared to third- and fourth-order Schrödinger equations. By maintaining the relative simplicity of the fourth-order Schrödinger equation, it is necessary to find other ways to relax the bandwidth restriction, while keeping the same order of correctness in nonlinearity.

Keeping this point in mind, Trulsen and Dysthe [29] investigated an evolution equation for broader bandwidth surface gravity waves on deep water, where the bandwidth and nonlinearity have been taken as $O(\epsilon^{1/2})$ and $O(\epsilon)$, respectively. Following Trulsen and Dysthe [29], in this paper, we have taken finite depth, deep water and infinite depth as $(kd)^{-1}$ being $O(1)$, $O(\epsilon)$ and 0, respectively, where k is the characteristic wavenumber and d denotes the depth of water.

According to Trulsen and Dysthe [29], one avenue of interest is to include some new linear terms to the fourth-order NLSE derived by Dysthe [10], which results in a remarkably better resolution in spectral bandwidth. The purpose of the present paper is to derive a new NLSE for a broader bandwidth and to develop a weakly nonlinear theory of periodic gravity-capillary waves on deep water in the presence of depth-uniform current. Therefore, the analysis of Trulsen and Dysthe is extended here to include the effects of both capillarity and depth-uniform current.

The paper is organized as follows. The framework for the problem is formulated in Section 1. Governing equations for water waves are given in Section 2. In Section 3, we present a new NLSE for broader bandwidth with a few results. Section 4 deals with the stability analysis and some important results and finally Section 5 concludes the paper.

2. Basic equations of water waves on a running stream

We choose an Eulerian frame $oxyz$, where oxy represents the plane coinciding with the undisturbed free surface of water and oz represents the z-axis along the vertically upward direction. Let $z = \alpha(x, y, t)$ be the equation of the free surface at any time

https://doi.org/10.1017/S1446181123000020 Published online by Cambridge University Press

t in the perturbed state. We assume that the waves are propagating steadily on a depth-uniform current U which is moving along the positive direction of the x-axis. The bottom of the uniform water depth is located at $y = -d$.

For an inviscid and incompressible flow of the fluid, we state the governing equations, free surface and the boundary condition of the water wave problem as

$$\nabla^2\phi = 0 \quad \text{in } -d < z < \alpha, \tag{2.1}$$

$$\phi_z - \alpha_t - U\alpha_x = \phi_x\alpha_x + \phi_y\alpha_y \quad \text{at } z = \alpha, \tag{2.2}$$

$$\phi_t + U\phi_x + g\alpha = -\frac{1}{2}(\nabla\phi)^2 + \frac{T}{\rho}(1 + \alpha_x^2 + \alpha_y^2)^{-3/2} \times (\alpha_x^2\alpha_{yy} + \alpha_y^2\alpha_{xx} - 2\alpha_x\alpha_y\alpha_{xy} + \alpha_{xx} + \alpha_{yy}) \quad \text{at } z = \alpha, \tag{2.3}$$

$$\phi_z = 0 \quad \text{at } z = -d, \tag{2.4}$$

where g is the acceleration due to gravity, ϕ is the perturbed velocity potential of waves, T is the surface tension coefficient, ρ is the density of water and $\nabla = (\partial/\partial x, \partial/\partial y, \partial/\partial z)$.

In view of nonlinear effects, the primary harmonic produces components given by the slow drift $\overline{\phi}$ and set down $\overline{\alpha}$, the second harmonics ϕ_2, α_2 and so on. Therefore, the solutions of the above equations can be expressed as

$$A = \overline{A} + \sum_{n=1}^{\infty}[A_n \exp\{in(kx - \sigma t)\} + c.c.], \quad (i = \sqrt{-1}), \tag{2.5}$$

in which A represents ϕ and α, $c.c.$ means complex conjugate of the previous term, and k, σ are the wavenumber and the frequency of the carrier wave, respectively. Now, $\overline{\phi}, \overline{\alpha}$, ϕ_n, α_n $(n = 1, 2, \ldots)$ and their complex conjugates are slowly varying functions on a time scale ϵt and space scale ϵx, ϵy, where ϵ denotes a slow ordering parameter measuring the weakness of nonlinearity. Further, as obtained from equation (3.6), $\overline{\phi}$ depends on the slow vertical variable ϵz, whereas ϕ_n $(n = 1, 2, \ldots)$ and their complex conjugates are functions of z (see [29]). Here, we consider the fourth-order NLEE for a narrow bandwidth describing the time evolution of α when the motion is weakly nonlinear, that is, $0 < \epsilon \ll 1$, subject to the following assumptions:

$$ka = O(\epsilon), \quad |\Delta\boldsymbol{k}|/k = O(\epsilon), \quad (kd)^{-1} = O(\epsilon).$$

It is important to note that the parameter ϵ describes both the slow modulations and the wave amplitude (see [12]). Herein, $\epsilon\alpha_1$ is the complex wave amplitude and, to leading first-order, the wave train is described by $\epsilon\alpha_1 \exp\{i(kx - \sigma t)\}$. So the first term on the right side of equation (3.5) corresponding to a narrow bandwidth is of the order of magnitude $O(\epsilon^3)$, whereas the remaining terms are of the order of magnitude $O(\epsilon^4)$, as the derivative increases the order by one.

The derivation of evolution equation requires that ϵ is a small parameter and describes the balance between nonlinearity and wave dispersion about the dominant

https://doi.org/10.1017/S1446181123000020 Published online by Cambridge University Press

wavenumber k. Typically, one assumes that the wave steepness and bandwidth are of the same order of magnitude $O(\epsilon)$, for which the nonlinear and dispersive effects balance at the fourth-order $O(\epsilon^4)$.

Subsequently, we assume that the waves are propagating along the x-direction and the linear dispersion relation for deep water gravity-capillary waves is given by

$$h(\sigma, k) = \sigma^2(1-u)^2 - kg(1+\kappa) = 0,$$

where $\kappa = Tk^2/(\rho g)$, the nondimensional surface tension coefficient, $u = U/c_p$ and $c_p = \sigma/k$ is the phase velocity of the carrier wave. Then the group velocity of the carrier wave becomes

$$\tilde{c}_g = \frac{c_g}{c_p} = \frac{2u + (1-u)((1+3\kappa)/(1+\kappa))}{2}.$$

3. The new Schrödinger equation for broader bandwidth

To obtain better resolution in wave bandwidth, following Trulsen and Dysthe [29], we take the assumptions given by

$$ka = O(\epsilon), \quad |\Delta \boldsymbol{k}|/k = O(\epsilon^{1/2}), \quad (kd)^{-1} = O(\epsilon^{1/2}).$$

We employ here the same harmonic expansions in equation (2.5) for the velocity potential ϕ and surface elevation α. In this case, $\overline{\phi}$, $\overline{\alpha}$, ϕ_n, α_n, $(n = 1, 2, \ldots)$, and their complex conjugates are functions of the slightly faster modulation variables on a time scale $\epsilon^{1/2}t$ and space scale $\epsilon^{1/2}x$, $\epsilon^{1/2}y$, and also $\overline{\phi}$ depends on the slightly faster variable $\epsilon^{1/2}z$.

Substituting the expansion for ϕ given by equation (2.5) in equation (2.1) and then equating the coefficients of $\exp\{in(kx - \sigma t)\}$ for $n = 1, 2, 0$, we get the following equations:

$$\frac{d^2\phi_n}{dz^2} - \Delta_n^2 \phi_n = 0, \tag{3.1}$$

where the operator Δ_n $(n = 1, 2)$ is given by

$$\Delta_n^2 = \left[\left(nk - i\epsilon^{1/2}\frac{\partial}{\partial x_1}\right)^2 - \epsilon\frac{\partial^2}{\partial y_1^2}\right].$$

The solutions of equation (3.1) satisfying the boundary condition in equation (2.4) can be put in the form

$$\phi_n = \frac{\cosh[(z+d)\Delta_n]}{\cosh(d\Delta_n)} B_n \quad \text{for } n = 1, 2, \tag{3.2}$$

$$\tilde{\overline{\phi}} = \frac{\cosh[\epsilon^{1/2}\tilde{k}(z+d)]}{\cosh(\epsilon^{1/2}\tilde{k}d)} \tilde{B}_0, \tag{3.3}$$

https://doi.org/10.1017/S1446181123000020 Published online by Cambridge University Press

where Δ_n operates on B_n $(n = 1, 2)$, which are functions of $x_1 = \epsilon^{1/2}x$, $y_1 = \epsilon^{1/2}y$, $t_1 = \epsilon^{1/2}t$. Here, $\tilde{\overline{\phi}}$ is the Fourier transform of $\overline{\phi}$ defined by

$$\tilde{\overline{\phi}} = \int\int\int_{-\infty}^{\infty} \overline{\phi}\, e^{i(\tilde{k}_x x_1 + \tilde{k}_y y_1 - \tilde{\sigma} t_1)}\, dx_1\, dy_1\, dt_1,$$

where $\tilde{k}^2 = \tilde{k}_x^2 + \tilde{k}_y^2$ and $\tilde{B}_0$ is a function of $\tilde{k}_x$, $\tilde{k}_y$ and $\tilde{\sigma}$.

On substituting the expansions in equation (2.5) in the Taylor-expanded form of equations (2.2) and (2.3) about $z = 0$ and then equating coefficients of $\exp\{in(kx - \sigma t)\}$ for $n = 1,\ 2,\ 0$ on both sides, we get three sets of equations, in each of which we substitute the solutions for ϕ_n and $\tilde{\overline{\phi}}$ given by equations (3.2) and (3.3), respectively. For convenience, we have taken the Fourier transform of the set of equations corresponding to $n = 0$. To solve the three sets of equations, we make the following perturbation expansion of the quantities $B_n,\ \alpha_n$ $(n = 1,\ 2,\ 0)$

$$F_1 = \sum_{n=1}^{\infty} \epsilon^n F_{1n}\,, \quad F_m = \sum_{n=2}^{\infty} \epsilon^n F_{mn}\ (m = 0,\ 2), \tag{3.4}$$

where F_j stands for B_j and α_j $(j = 1,\ 2,\ 0)$.

Here, we maintain the same order of correctness in nonlinearity as in the fourth-order evolution equation for narrow bandwidth, and note that since all the fourth-order contributions to this equation are not quartically nonlinear, it is enough to consider the new Schrödinger equation for broader bandwidth only up to $O(\epsilon^{3.5})$.

It is helpful to use dimensionless variables by introducing the substitutions

$$\sigma t \to \sigma, \quad k(\alpha,\ x,\ y,\ z) \to (\alpha,\ x,\ y,\ z), \quad \frac{k^2}{\sigma}\,\overline{\phi} \to \overline{\phi}.$$

Carrying out the perturbation analysis by a standard procedure due to Dhar and Das [8], we obtain the coupled nonlinear Schrödinger equations for broader bandwidth in terms of α $(\alpha = \epsilon\alpha_{11} + \epsilon^2\alpha_{12},\ \alpha_{11}$ and α_{12} being the first two terms in the perturbation expansion in equation (3.4) of α_1 in powers of $\epsilon)$ and $\overline{\phi}$ as follows:

$$\begin{aligned} &i\left(\frac{\partial\alpha}{\partial t} + c_g\frac{\partial\alpha}{\partial x}\right) - \gamma_1\frac{\partial^2\alpha}{\partial x^2} + \gamma_2\frac{\partial^2\alpha}{\partial y^2} + i\left(\gamma_3\frac{\partial^3\alpha}{\partial x^3} + \gamma_4\frac{\partial^3\alpha}{\partial x\partial y^2}\right) + \gamma_5\frac{\partial^4\alpha}{\partial x^4} \\ &\quad + \gamma_6\frac{\partial^4\alpha}{\partial x^2\partial y^2} + \gamma_7\frac{\partial^4\alpha}{\partial y^4} + i\left(\gamma_8\frac{\partial^5\alpha}{\partial x^5} + \gamma_9\frac{\partial^5\alpha}{\partial x^3\partial y^2} + \gamma_{10}\frac{\partial^5\alpha}{\partial x\partial y^4}\right) \\ &\quad = \mu_1|\alpha|^2\alpha + i\left(\mu_2|\alpha|^2\frac{\partial\alpha}{\partial x} + \mu_3\alpha^2\frac{\partial\alpha^*}{\partial x}\right) + \alpha\frac{\partial\overline{\phi}}{\partial x} \quad \text{at } z = 0, \end{aligned} \tag{3.5}$$

$$\nabla^2\overline{\phi} = 0 \quad \text{in} - d < z < 0,$$

$$\frac{\partial\overline{\phi}}{\partial z} = 2\frac{\partial}{\partial x}(|\alpha|^2) \quad \text{at } z = 0, \tag{3.6}$$

$$\frac{\partial\overline{\phi}}{\partial z} = 0 \quad \text{at } z = -d, \tag{3.7}$$

https://doi.org/10.1017/S1446181123000020 Published online by Cambridge University Press

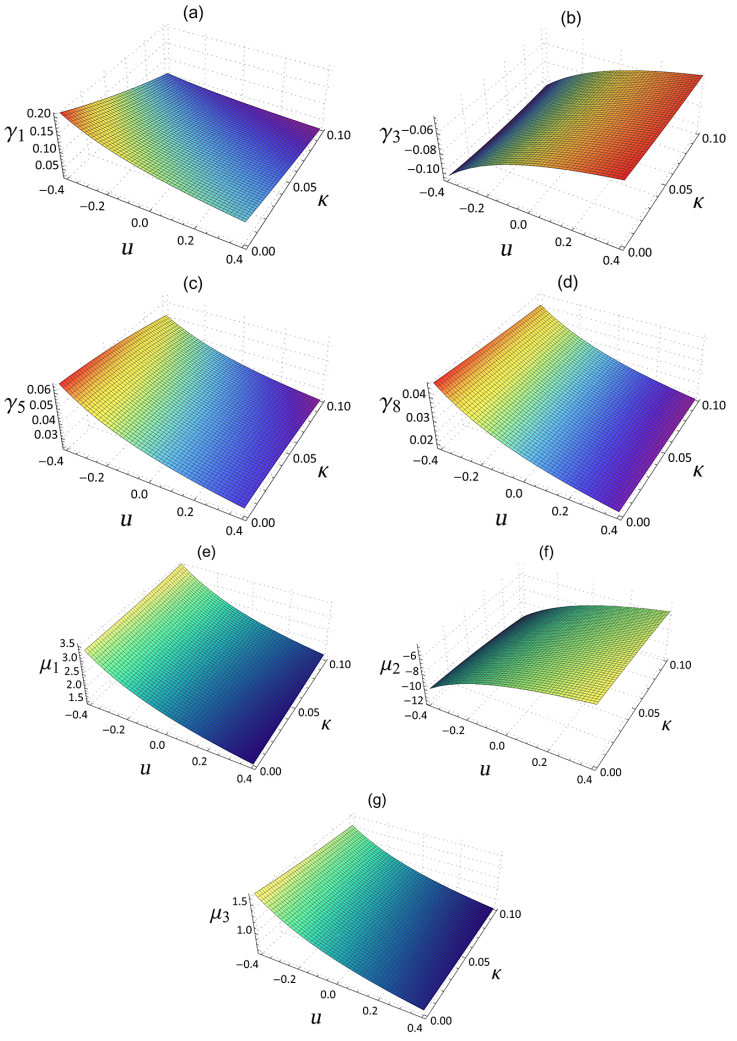

FIGURE 1. Dimensionless coefficients of a new NLSE as functions of u and κ.

where "$*$" indicates the complex conjugate; the coefficients appearing in equation (3.5) are given in Appendix A.

In the new Schrödinger equation (3.5) for broader bandwidth, we have assumed that the wave steepness is of the order $O(\epsilon)$, whereas the bandwidth is of the order $O(\epsilon^{1/2})$ for which the nonlinear and dispersive effects balance at the order of $O(\epsilon^{3.5})$.

In the absence of capillarity and depth-uniform current, equation (3.5) reduces to an equation equivalent to of Trulsen and Dysthe [29, equation (21)].

Figure 1 exhibits the variations of different nondimensional coefficients of dispersive and nonlinear terms of a new NLSE given by equation (3.5) as functions of u

https://doi.org/10.1017/S1446181123000020 Published online by Cambridge University Press

and κ. From this figure, it is found that both uniform current and surface tension have a considerable effect on these coefficients.

4. Modulational instability analysis and results

A solution of the coupled nonlinear Schrödinger equations is given by

$$\alpha = \frac{\alpha_0}{2}\exp(-i\Delta\sigma t), \quad \overline{\phi} = \phi_0,$$

where α_0 and ϕ_0 are real constants and the frequency shift is

$$\Delta\sigma = \frac{\mu_1}{4}\alpha_0^2.$$

We assume the perturbation on this solution as follows:

$$\alpha = \frac{\alpha_0}{2}(1+\alpha')\exp\{i(\theta' - \Delta\sigma t)\}, \quad \overline{\phi} = \phi_0 + \phi', \tag{4.1}$$

where α', θ' are small real perturbations of amplitude and phase, respectively, and ϕ' is a real small perturbation of $\overline{\phi}$. Inserting equation (4.1) in equation (3.5), the linearized version of this equation can be simplified to

$$R_1\alpha' + R_2\theta' - \frac{(\mu_2+\mu_3)}{4}\alpha_0^2\frac{\partial\alpha'}{\partial x} = 0 \quad \text{at } z = 0, \tag{4.2}$$

$$R_2\alpha' - R_1\theta' - \frac{\mu_1}{2}\alpha_0^2\alpha' + \frac{(\mu_2-\mu_3)}{4}\alpha_0^2\frac{\partial\theta'}{\partial x} - \frac{\partial\phi'}{\partial x} = 0 \quad \text{at } z = 0, \tag{4.3}$$

where

$$R_1 = \frac{\partial}{\partial t} + c_g\frac{\partial}{\partial x} + \gamma_3\frac{\partial^3}{\partial x^3} + \gamma_4\frac{\partial^3}{\partial x\partial y^2} + \gamma_8\frac{\partial^5}{\partial x^5} + \gamma_9\frac{\partial^5}{\partial x^3\partial y^2} + \gamma_{10}\frac{\partial^5}{\partial x\partial y^4},$$
$$R_2 = -\gamma_1\frac{\partial^2}{\partial x^2} + \gamma_2\frac{\partial^2}{\partial y^2} + \gamma_5\frac{\partial^4}{\partial x^4} + \gamma_6\frac{\partial^4}{\partial x^2\partial y^2} + \gamma_7\frac{\partial^4}{\partial y^4}.$$

The linearized version of equation (3.6) can be expressed as

$$\frac{\partial\phi'}{\partial z} = \alpha_0^2\frac{\partial\alpha'}{\partial x} \quad \text{at } z = 0. \tag{4.4}$$

From equations (3.7) and (4.1), we also have

$$\frac{\partial\phi'}{\partial z} = 0 \quad \text{at } z = -d. \tag{4.5}$$

Now using equation (4.5), we take the plane wave solution of the above equations (4.2), (4.3) and (4.4) given by

https://doi.org/10.1017/S1446181123000020 Published online by Cambridge University Press

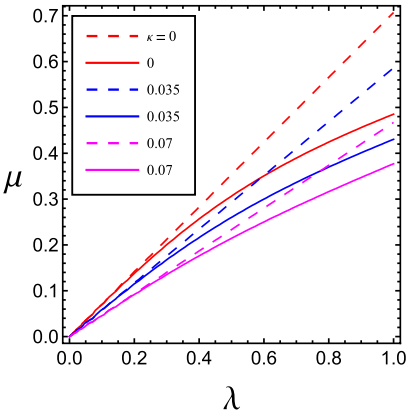

FIGURE 2. The stability curves in the limit $\alpha_0 = 0$ in the (λ, μ) plane for $u = 0$ and several values of κ. Solid lines show the new broader-banded results, dashed lines show the narrow-banded results.

$$\begin{pmatrix} \alpha' \\ \theta' \end{pmatrix} = \begin{pmatrix} \hat{\alpha} \\ \hat{\theta} \end{pmatrix} \exp\{i(\lambda x + \mu y - \Omega t)\} + c.c.,$$

$$\phi' = \hat{\phi}[\exp\{i(\lambda x + \mu y - \Omega t)\} + c.c.] \frac{\cosh \overline{k}(z + d)}{\cosh(\overline{k} d)},$$

where $\overline{k}^2 = \lambda^2 + \mu^2$.

The perturbed wavenumbers λ, μ and the perturbed frequency Ω satisfy the nonlinear dispersion relation

$$\left[\overline{R}_1 + \frac{(\mu_2 + \mu_3)}{4}\alpha_0^2\lambda\right]\left[\overline{R}_1 + \frac{(\mu_2 - \mu_3)}{4}\alpha_0^2\lambda\right] = \overline{R}_2\left[\overline{R}_2 - \frac{\mu_1}{2}\alpha_0^2 + \frac{\alpha_0^2\lambda^2}{\overline{k}\tanh(\overline{k}d)}\right], \tag{4.6}$$

where

$$\overline{R}_1 = \Omega - c_g\lambda + \gamma_3\lambda^3 + \gamma_4\lambda\mu^2 - \gamma_8\lambda^5 - \gamma_9\lambda^3\mu^2 - \gamma_{10}\lambda\mu^4, \tag{4.7}$$

$$\overline{R}_2 = \gamma_1\lambda^2 - \gamma_2\mu^2 + \gamma_5\lambda^4 + \gamma_6\lambda^2\mu^2 + \gamma_7\mu^4. \tag{4.8}$$

A salient feature of the new broader-banded equation is that the neutral stability curves, as displayed in Figure 2, in the limit $\alpha_0 = 0$ are no longer straight lines. Note that the fourth-order NLEE corresponding to narrow bandwidth has neutral stability along the intersecting straight lines $\gamma_1\lambda^2 - \gamma_2\mu^2 = 0$ (obtained from equation (4.16)) for $\alpha_0 = 0$. In the new broader-banded theory, the corresponding neutral stability curves are obtained from $\overline{R}_2 = 0$ given by equation (4.8), which agree fairly well with the exact curves of Phillips [23] for large depth and moderate values of λ, μ.

https://doi.org/10.1017/S1446181123000020 Published online by Cambridge University Press

The solution of equation (4.6) is given by

$$\overline{R}_1 = -\frac{\mu_2}{4}\alpha_0^2\lambda \pm \sqrt{\overline{R}_2\left[\overline{R}_2 - \frac{\mu_1}{2}\alpha_0^2 + \frac{\alpha_0^2\lambda^2}{\overline{k}\tanh(\overline{k}d)}\right] + \frac{\mu_3^2}{16}\alpha_0^4\lambda^2}. \tag{4.9}$$

Using equation (4.7), we can write equation (4.9) as

$$\Omega = c_g\lambda - \gamma_3\lambda^3 - \gamma_4\lambda\mu^2 + \gamma_8\lambda^5 + \gamma_9\lambda^3\mu^2 + \gamma_{10}\lambda\mu^4 - \frac{\mu_2}{4}\alpha_0^2\lambda \pm \sqrt{\overline{R}_2\left[\overline{R}_2 - \frac{\mu_1}{2}\alpha_0^2 + \frac{\alpha_0^2\lambda^2}{\overline{k}\tanh(\overline{k}d)}\right] + \frac{\mu_3^2}{16}\alpha_0^4\lambda^2}. \tag{4.10}$$

From equation (4.10), the instability occurs if

$$\overline{R}_2\left[\overline{R}_2 - \frac{\mu_1}{2}\alpha_0^2 + \frac{\alpha_0^2\lambda^2}{\overline{k}\tanh(\overline{k}d)}\right] + \frac{\mu_3^2}{16}\alpha_0^4\lambda^2 < 0. \tag{4.11}$$

If the condition in equation (4.11) is satisfied, the perturbed frequency Ω will be complex valued, and the growth rate of instability represented by the imaginary part Ω_i of Ω becomes

$$\Omega_i = \sqrt{\overline{R}_2\left[\frac{\mu_1}{2}\alpha_0^2 - \overline{R}_2 - \frac{\alpha_0^2\lambda^2}{\overline{k}\tanh(\overline{k}d)}\right] - \frac{\mu_3^2}{16}\alpha_0^4\lambda^2}. \tag{4.12}$$

For $\mu = 0$, the instability condition and the growth rate Ω_i reduce respectively to

$$(\gamma_1\lambda^2 + \gamma_5\lambda^4)\left[\gamma_1\lambda^2 + \gamma_5\lambda^4 - \frac{\mu_1}{2}\alpha_0^2 + \frac{\alpha_0^2|\lambda|}{\tanh(d\lambda)}\right] + \frac{\mu_3^2}{16}\alpha_0^4\lambda^2 < 0,$$

$$\Omega_i = \sqrt{(\gamma_1\lambda^2 + \gamma_5\lambda^4)\left[\frac{\mu_1}{2}\alpha_0^2 - \gamma_1\lambda^2 - \gamma_5\lambda^4 - \frac{\alpha_0^2|\lambda|}{\tanh(d\lambda)}\right] - \frac{\mu_3^2}{16}\alpha_0^4\lambda^2}. \tag{4.13}$$

The instability regions obtained from equations (4.11) and (4.17) corresponding to broader bandwidth and narrow bandwidth, respectively, for depth $d = 6$ and wave steepness $\alpha_0 = 0.1, 0.2$, are shown in Figures 3 and 4. Figure 3(a) for $u = 0$, $\kappa = 0$ is identical with [29, Figure 5]. Thus, we can verify that this limiting case is reproduced properly.

Figures 5 and 6 show the modulational instability regions obtained from equations (4.11) and (4.17) for $\alpha_0 = 0.2$ and 0.4, respectively, in the case of an infinite depth of water. The region bounded by the solid line corresponding to new broader-banded result of Figure 5(a) for $u = 0, \kappa = 0, \alpha_0 = 0.2$ is found to nearly overlap with the region obtained from numerical computation of McLean et al. [21, Figure 1(a)]. Therefore, we conclude that the new NLSE for broader bandwidth gives excellent long wavelength two-dimensional instability regions for finite but small wave steepness.

https://doi.org/10.1017/S1446181123000020 Published online by Cambridge University Press

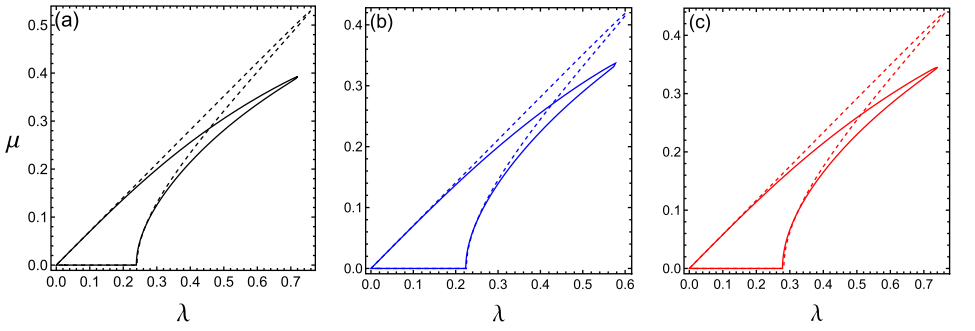

FIGURE 3. The (λ, μ) instability diagrams for $d = 6$ and $\alpha_0 = 0.1$: (a) $u = 0,\ \kappa = 0$; (b) $u = 0.4,\ \kappa = 0$; (c) $u = 0,\ \kappa = 0.035$. Solid lines show the new broader-banded result, dashed lines show the narrow-banded result.

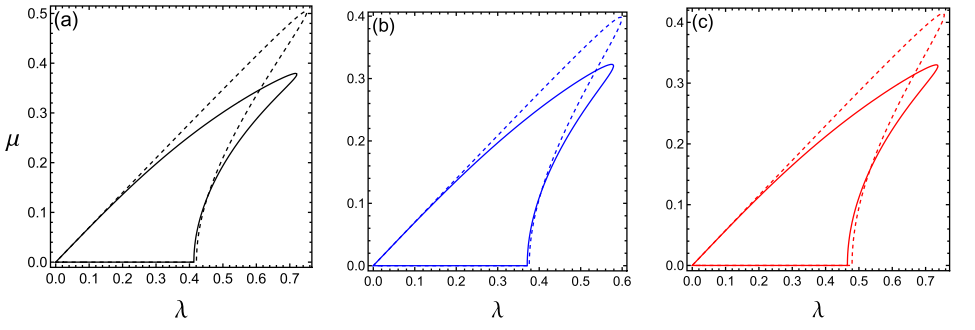

FIGURE 4. The (λ, μ) instability diagrams for $d = 6$ and $\alpha_0 = 0.2$: (a) $u = 0,\ \kappa = 0$; (b) $u = 0.4,\ \kappa = 0$; (c) $u = 0,\ \kappa = 0.035$. Solid lines show the new broader-banded results, dashed lines show the narrow-banded results.

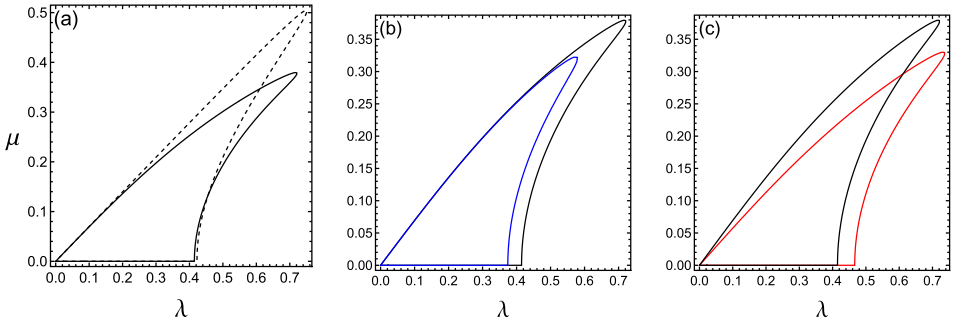

FIGURE 5. The (λ, μ) instability diagrams for infinite depth of water and $\alpha_0 = 0.2$: (a) $u = 0, \kappa = 0$, solid line shows the new broader-banded result, dashed line shows the narrow-banded result. Instability regions for new broader-banded result: (b) $\kappa = 0$, black line shows $u = 0$, blue line shows $u = 0.4$; (c) $u = 0$, black line shows $\kappa = 0$, red line shows $\kappa = 0.035$. (Colour available online.)

https://doi.org/10.1017/S1446181123000020 Published online by Cambridge University Press

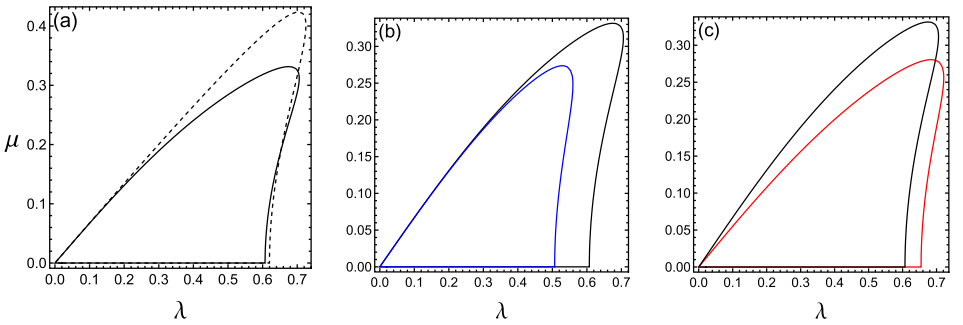

FIGURE 6. The (λ, μ) instability diagrams for infinite depth of water and $\alpha_0 = 0.4$: (a) $u = 0, \kappa = 0$, solid line shows the new broader-banded result, dashed line shows the narrow-banded result. Instability regions for new broader-banded result: (b) $\kappa = 0$, black line shows $u = 0$, blue line shows $u = 0.4$; (c) $u = 0$, black line shows $\kappa = 0$, red line shows $\kappa = 0.035$. (Colour available online.)

From these figures, we have observed a significant change of the instability regions obtained from broader-banded and narrow-banded results. It is also found that both depth-uniform current and surface tension have a small effect on the instability regions. Furthermore, the instability regions become wider with the increase of α_0.

In Figure 7, the contour plots of the growth rate of modulational instability Ω_i given by equation (4.13) in the (λ, u) plane have been plotted for $d = 6$ and two values of κ and α_0. We observe that the depth-uniform adverse current increases the growth rate, whereas the following current decreases the growth rate. Further, the growth rate increases with the increase of wave steepness. It is also found that the effect of capillarity is to decrease the growth rate giving a stabilizing influence.

Figures 8–11 show contour plots of instability growth rate Ω_i given by equation (4.12) in the (λ, μ) plane for $d = 6$ and several values of u, κ and α_0 corresponding to the new broader-banded result. We have shown that the growth rate decreases with the increase of both u and κ, whereas it increases with the increase of α_0. Further, depth-uniform opposing current increases the growth rate. We have also noticed a small change in the shape and span of the contour plots along both the axes.

Results for fourth-order NLEE on deep water corresponding to narrow bandwidth may be obtained from equation (3.5) by ignoring the fourth- and fifth-order derivative terms and are given by

$$\Omega = c_g\lambda - \gamma_3\lambda^3 - \gamma_4\lambda\mu^2 - \frac{\mu_2}{4}\alpha_0^2\lambda \pm \sqrt{P}, \tag{4.14}$$

where

$$P = \overline{S}\left[\overline{S} - \frac{\mu_1}{2}\alpha_0^2 + \frac{\alpha_0^2\lambda^2}{\overline{k}\tanh(\overline{k}d)}\right] + \frac{\mu_3^2}{16}\alpha_0^4\lambda^2, \tag{4.15}$$

$$\overline{S} = \gamma_1\lambda^2 - \gamma_2\mu^2. \tag{4.16}$$

https://doi.org/10.1017/S1446181123000020 Published online by Cambridge University Press

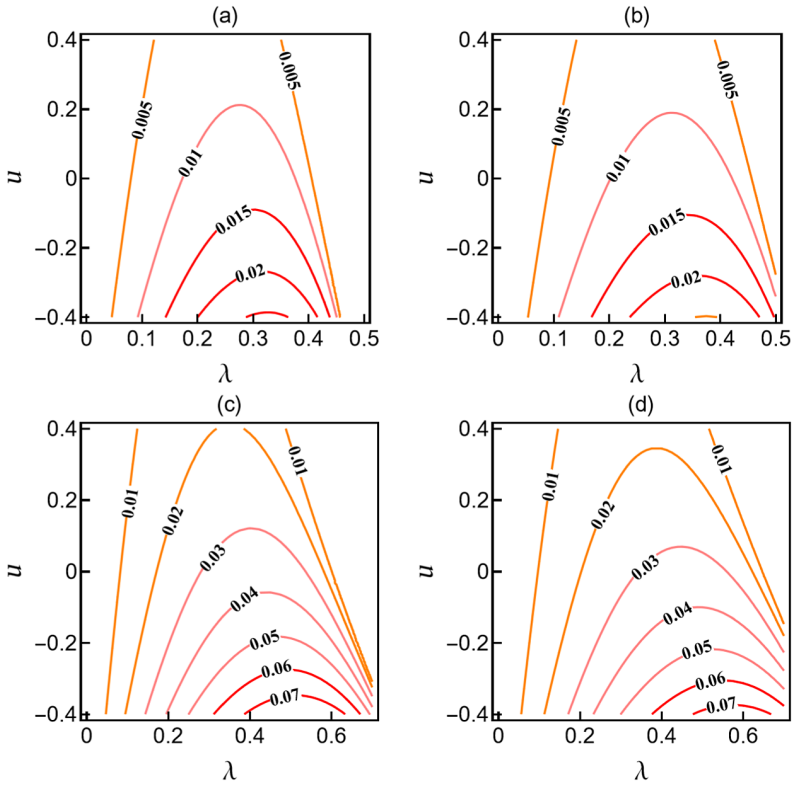

FIGURE 7. Contour plots of growth rate $\Omega_i(\lambda, u)$ for $d = 6$. $\alpha_0 = 0.2$: (a) $\kappa = 0$; (b) $\kappa = 0.035$. $\alpha_0 = 0.4$: (c) $\kappa = 0$; (d) $\kappa = 0.035$.

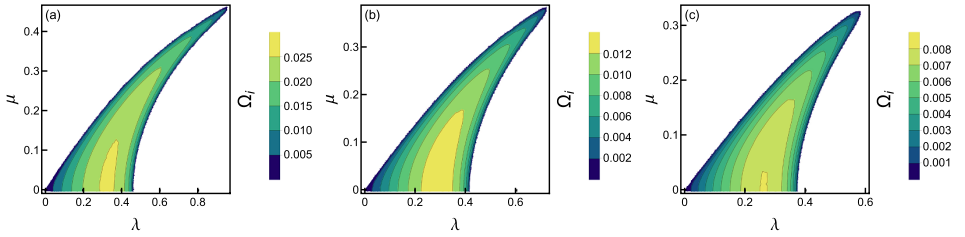

FIGURE 8. Contour plots of growth rate $\Omega_i(\lambda, \mu)$ corresponding to new broader-banded result for $d = 6$, $\alpha_0 = 0.2$, $\kappa = 0$: (a) $u = -0.4$; (b) $u = 0$; (c) $u = 0.4$.

It is important to note that in equation (4.15), the last term $(\mu_3^2\alpha_0^4\lambda^2)/16$ corresponding to the nonlinear term $i\mu_3\alpha^2(\partial\alpha^*/\partial x)$ of equation (3.5) is insignificant within the fourth-order $O(\epsilon^4)$, and has been often neglected in preceding works [7, 10]. However, the actual behaviour of the evolution equation corresponding to narrow bandwidth is described by the full expression of equation (4.15). Considering the last term in

https://doi.org/10.1017/S1446181123000020 Published online by Cambridge University Press

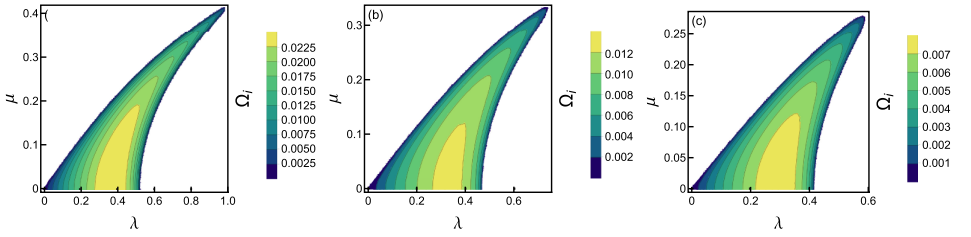

FIGURE 9. Contour plots of growth rate $\Omega_i(\lambda, \mu)$ corresponding to new broader-banded result for $d = 6$, $\alpha_0 = 0.2$, $\kappa = 0.035$: (a) $u = -0.4$; (b) $u = 0$; (c) $u = 0.4$.

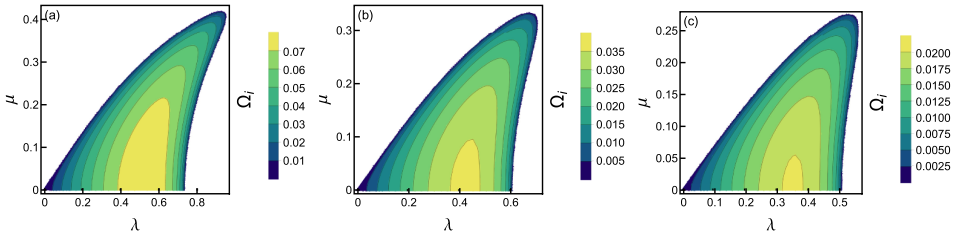

FIGURE 10. Contour plots of growth rate $\Omega_i(\lambda, \mu)$ corresponding to new broader-banded result for $d = 6$, $\alpha_0 = 0.4$, $\kappa = 0$: (a) $u = -0.4$; (b) $u = 0$; (c) $u = 0.4$.

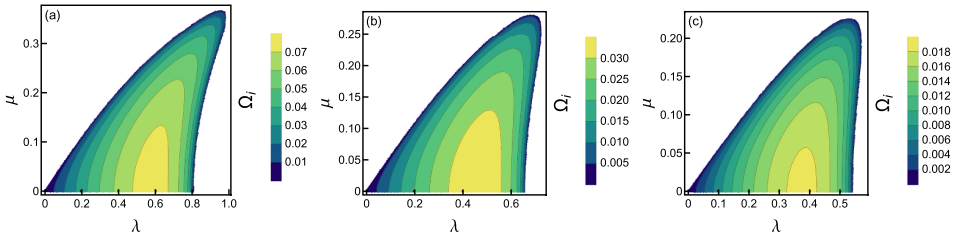

FIGURE 11. Contour plots of growth rate $\Omega_i(\lambda, \mu)$ corresponding to new broader-banded result for $d = 6$, $\alpha_0 = 0.4$, $\kappa = 0.035$: (a) $u = -0.4$; (b) $u = 0$; (c) $u = 0.4$.

equation (4.15) according to Trulsen and Dysthe [29], we have observed that its effect is to reduce the extent of the instability region, as shown in Figure 12. As a check, the primary instability regions we obtain in Figure 12(a) for $u = 0$, $\kappa = 0$ are compared with those obtained by Trulsen and Dysthe [29, Figure 1]. Thus, we can verify that the limiting case is reproduced exactly. Moreover, importance has been attached to the nonlinear term $i\mu_2|\alpha|^2(\partial\alpha/\partial x)$ of the NLSE in equation (3.5). We find from equation (4.14) that it provides the real $O(\alpha_0^2)$ correction to the frequency of sufficiently large plane wave perturbations.

From equation (4.14), the instability occurs if

$$\overline{S}\left[\overline{S} - \frac{\mu_1}{2}\alpha_0^2 + \frac{\alpha_0^2\lambda^2}{\overline{k}\tanh(\overline{k}d)}\right] + \frac{\mu_3^2}{16}\alpha_0^4\lambda^2 < 0. \tag{4.17}$$

https://doi.org/10.1017/S1446181123000020 Published online by Cambridge University Press

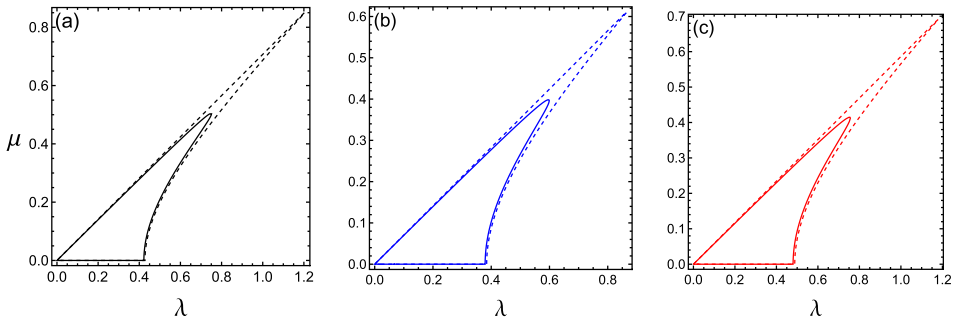

FIGURE 12. The (λ, μ) instability diagrams for infinite depth and $\alpha_0 = 0.2$: (a) $u = 0,\ \kappa = 0$; (b) $u = 0.4,\ \kappa = 0$; (c) $u = 0,\ \kappa = 0.035$. Solid lines are based on the full expression of equation (4.15), dashed lines are based on the expression in equation (4.15) excluding the last term.

If the condition in equation (4.17) is satisfied, the perturbed frequency Ω will be complex valued and the growth rate of instability represented by the imaginary part Ω_i of Ω becomes

$$\Omega_i = \sqrt{\overline{S}\left[\frac{\mu_1}{2}\alpha_0^2 - \overline{S} - \frac{\alpha_0^2\lambda^2}{\overline{k}\tanh(\overline{k}d)}\right] - \frac{\mu_3^2}{16}\alpha_0^4\lambda^2}. \tag{4.18}$$

In the case of one-dimensional perturbation $\mu = 0$, equations (4.17) and (4.18) reduce respectively to

$$\gamma_1\left[\gamma_1\lambda^2 - \frac{\mu_1}{2}\alpha_0^2 + \frac{\alpha_0^2|\lambda|}{\tanh(d\lambda)}\right] + \frac{\mu_3^2}{16}\alpha_0^4 < 0, \tag{4.19}$$

$$\Omega_i = \lambda\sqrt{\gamma_1\left[\frac{\mu_1}{2}\alpha_0^2 - \gamma_1\lambda^2 - \frac{\alpha_0^2|\lambda|}{\tanh(d\lambda)}\right] - \frac{\mu_3^2}{16}\alpha_0^4}. \tag{4.20}$$

Omitting last term of equation (4.19), it becomes

$$\gamma_1^2\lambda^2 - \frac{\gamma_1}{2}\left[\mu_1 - \frac{2|\lambda|}{\tanh(d\lambda)}\right]\alpha_0^2 < 0. \tag{4.21}$$

Note that in the absence of depth-uniform current, instability is possible when

$$(2\kappa - 1)(3\kappa^2 + 6\kappa - 1) > 0,$$

from which the ranges of κ are given by

$$0 < \kappa < (2/\sqrt{3} - 1) = 0.1547, \quad 0.5 < \kappa < \infty.$$

These results are in agreement with the results obtained by Zakharov [32]. Herein, the value 0.1547 of κ corresponds to the minimum group velocity and the value 0.5 of κ to the first Wilton [31] ripple.

https://doi.org/10.1017/S1446181123000020 Published online by Cambridge University Press

For infinite depth, the expression for maximum growth rate of instability becomes

$$G_m = \frac{|\mu_1|}{4}\left[1 - \frac{1}{\mu_1}\left(\frac{\mu_1}{\gamma_1}\right)^{\frac{1}{2}}\alpha_0\right]\alpha_0^2, \tag{4.22}$$

which occurs for the wavenumber

$$\lambda_m = \frac{1}{2}\left[\sqrt{\frac{\mu_1}{\gamma_1}} - \frac{3}{4\gamma_1}\alpha_0\right]\alpha_0.$$

For $u = 0$, G_m takes the form

$$G_m = \frac{1}{16}\left[1 + \frac{8}{\sqrt{6}}\alpha_0\right]\alpha_0^2 \tag{4.23}$$

in the case of pure capillary waves, and reduces to

$$G_m = \tfrac{1}{2}[1 + \tfrac{9}{8}\kappa - 2(1 + \tfrac{73}{16}\kappa)\alpha_0]\alpha_0^2, \tag{4.24}$$

when κ is small.

The expressions for G_m given by equations (4.23) and (4.24) are identical with Hogan's [14, equations (3.16b) and (3.16c)], respectively. It is important to note that the correction to the maximum growth rate in equation (4.22) is of fourth-order, involving three terms, namely, the frequency-dispersion term, the nonlinear term and the mean flow term. Since the frequency-dispersion term for pure capillary waves is of opposite sign of pure gravity waves, so too are the corrections to the stability properties.

From equation (4.21), the instability bandwidth for infinite depth is given by

$$\lambda = \left[\sqrt{\frac{\mu_1}{2\gamma_1}} - \frac{1}{2\gamma_1}\alpha_0\right]\alpha_0.$$

At marginal stability, Ω_r, the real part of Ω then becomes

$$\Omega_r = c_g\left[\sqrt{\frac{\mu_1}{2\gamma_1}} - \frac{1}{2\gamma_1}\alpha_0\right]\alpha_0. \tag{4.25}$$

Further, the value of the real part of Ω corresponding to λ_m is

$$\Omega_{rm} = \frac{c_g}{2}\left[\sqrt{\frac{\mu_1}{\gamma_1}} - \frac{3}{4\gamma_1}\alpha_0\right]\alpha_0. \tag{4.26}$$

Result for the third-order Schrödinger equation analysis on infinite depth has been given previously by Liao et al. [17] for $\Omega = 0$, and may be obtained from equation (4.20) by omitting the fourth-order terms and setting $\kappa = 0$, and it is given by

$$\frac{\Omega_i}{\alpha_0^2} = \frac{\lambda}{\alpha_0}\sqrt{\frac{\gamma_1\mu_1}{2} - \gamma_1^2\left(\frac{\lambda}{\alpha_0}\right)^2}. \tag{4.27}$$

The maximum growth rate of instability G_m given by equation (4.22) is shown in Figure 13 as a function of wave steepness α_0 for some values of u and κ. For $u = 0$,

https://doi.org/10.1017/S1446181123000020 Published online by Cambridge University Press

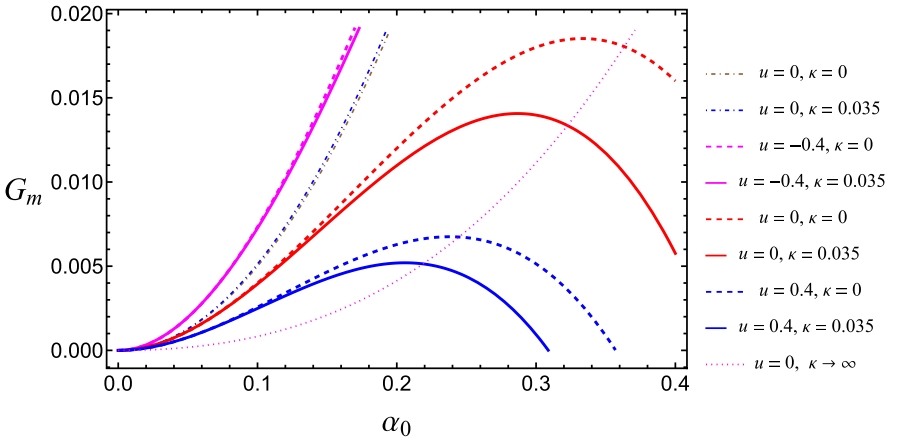

FIGURE 13. Plot of G_m versus α_0 for several values of u and κ. Solid, dashed and dotted lines show the fourth-order results, dash–dotted lines show the third-order results.

$\kappa = 0$, the red dashed curve obtained from the fourth-order result nearly overlaps with the curve for class I, $m = 1$ of McLean [20, Figure 6]. So we find an excellent agreement with the exact numerical result of McLean [20]. As described by McLean, the class I, $m = 1$ instability has a growth rate of second-order of wave steepness for small wave steepness, which is in agreement with the perturbation analysis of Benjamin and Feir [1]. It is also seen from Figure 13 that the maximum growth rate obtained from the fourth-order result first increases with α_0 and then decreases, while the growth rate G_m computed from the third-order result (shown as dash–dotted line) increases steadily with α_0. The depth-uniform following current first increases and then decreases the modulational instability, whereas an opposing current significantly increases the growth rate. In the absence of depth-uniform current, we observe a significant change of the maximum growth rate obtained from equations (4.23) and (4.24) for pure capillary waves ($\kappa \to \infty$, shown as a dotted line) and pure gravity waves ($\kappa = 0$, shown as a red dashed line), respectively, due to the sign change of the frequency-dispersion term. Further, the effect of surface tension is to decrease the growth rate of instability.

In Figure 14, the ratio of the maximum growth rate of instability to its value in the absence of capillarity corresponding to the third-order result obtained from equation (4.22) has been plotted against κ for different values of depth-uniform current u. We observe that the effects of both capillarity and depth-uniform current are to increase steadily the maximum growth rate.

The perturbed frequency Ω_r at marginal stability given by equation (4.25) has been plotted in Figure 15 against α_0 for different values of u and κ. For $u = 0$, $\kappa = 0$, it is observed that equation (4.25) is fairly close to the exact results of Longuet-Higgins [18] for $\alpha_0 < 0.3$. In Figure 16, the contour plots of $\Omega_{rm}(\alpha_0, u)$ given by equation (4.26) have been plotted for two values of κ.

https://doi.org/10.1017/S1446181123000020 Published online by Cambridge University Press

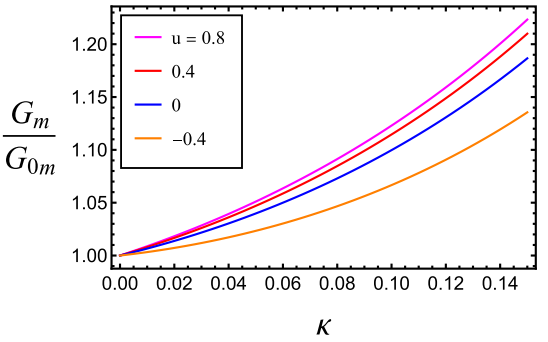

FIGURE 14. Normalized maximum growth rate versus κ for some values of u.

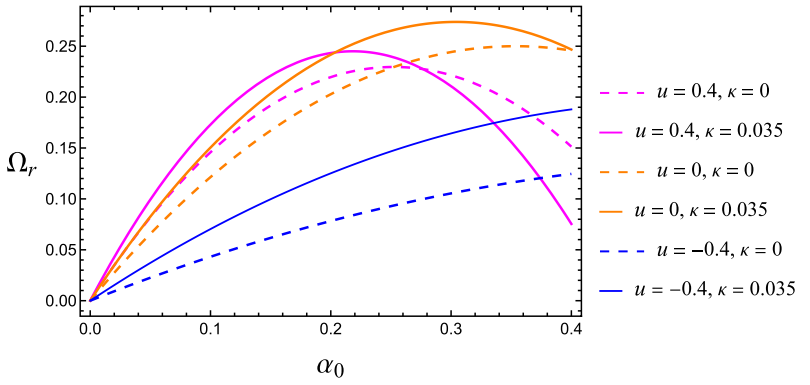

FIGURE 15. Curves of marginal stability versus α_0 for some values of u and κ.

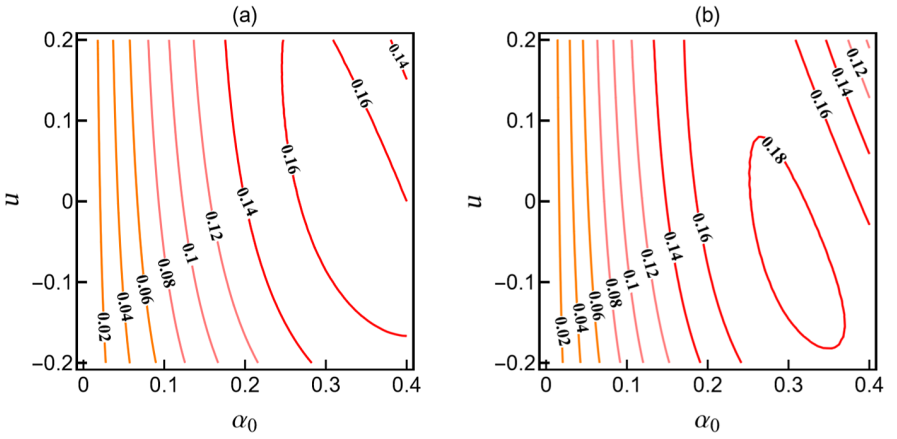

FIGURE 16. Contour plots of frequency separation of fastest growing sideband $\Omega_{rm}(\alpha_0, u)$: (a) $\kappa = 0$; (b) $\kappa = 0.035$.

https://doi.org/10.1017/S1446181123000020 Published online by Cambridge University Press

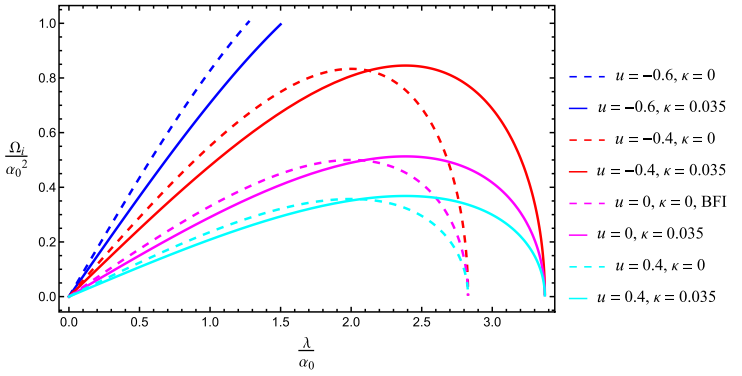

FIGURE 17. Plot of growth rate of instability Ω_i/α_0^2 versus λ/α_0 for several values of u and κ. BFI refers to the Benjamin–Feir instability.

Figure 17 shows the growth rate Ω_i/α_0^2 given by equation (4.27) as a function of λ/α_0 at different values of u and κ. We find that the depth-uniform adverse current can largely expand the onset criterion and significantly enhances the instability growth rate, whereas the depth-uniform following current decreases the growth rate, consistent with the result of Liao et al. [17]. Furthermore, the influence of the capillary is to depress the instability growth rate due to modulation.

5. Conclusion

Using the multiple scale method, a current modified NLSE for broader bandwidth gravity-capillary waves on deep water is investigated. The inclusion of a few new linear terms to the NLSE corresponding to narrow bandwidth has considerably improved the resolution in spectral bandwidth. By the improved resolution in spectral bandwidth, the new equation may satisfy the major objection against using the band-restricted Schrödinger equation for numerical calculations on three-dimensional weakly nonlinear water-surface waves. With the new Schrödinger equation, the extent of the instability region of a Stokes wave has been reduced. Therefore, the results of the stability analysis for uniform Stokes waves based on the new broader-banded equation are superior to those based on the narrow-banded equation, and they agree fairly well with the exact numerical computations of McLean [20] and McLean et al. [21]. We therefore expect that the new equation has sufficient bandwidth to be effective for realistic ocean wave problems.

Acknowledgment

The authors are grateful to the reviewers for their useful comments to improve the manuscript.

https://doi.org/10.1017/S1446181123000020 Published online by Cambridge University Press

Appendix A. Coefficients appearing in equation (3.5)

$$\gamma_1 = \frac{B}{2h_\sigma^2(1+\kappa)}, \quad \gamma_2 = \frac{1+3\kappa}{h_\sigma^2}, \quad \gamma_3 = \frac{2AB - \kappa h_\sigma^4}{2h_\sigma^4(1+\kappa)},$$

$$\gamma_4 = \frac{(1-3\kappa)h_\sigma^2 - 2(1+3\kappa)A}{4h_\sigma^2(1+\kappa)}, \quad \gamma_5 = \frac{A^4 + 4A^2B - 6A^2\kappa h_\sigma^2 - 2A\kappa h_\sigma^4 + 9\kappa^2 h_\sigma^2}{2h_\sigma^6(1+\kappa)},$$

$$\gamma_6 = \frac{(1-3\kappa)Ah_\sigma^2 - (1+3\kappa)(2A^2+B) - (h_\sigma^4/2)}{2h_\sigma^4(1+\kappa)}, \quad \gamma_7 = \frac{2(1+3\kappa)^2 + (1-3\kappa)h_\sigma^2}{16h_\sigma^2(1+\kappa)},$$

$$\gamma_8 = \frac{-2AB(4A^2+3B) + 4B\kappa h_\sigma^4 + 4uA\kappa h_\sigma^5 + 2\{h_k^2 - (u^2-3\kappa)h_\sigma^2\}\kappa h_\sigma^4}{2h_\sigma^8(1+\kappa)},$$

$$\gamma_9 = \frac{(1+3\kappa)(4A^3 + 6AB - \kappa h_\sigma^4) - (1-3\kappa)(2A^2h_\sigma^2 + Bh_\sigma^2) + Ah_\sigma^4 - (h_\sigma^6/2)}{2h_\sigma^6(1+\kappa)},$$

$$\gamma_{10} = \frac{-2(1-3\kappa)Ah_\sigma^2 - 12(1+3\kappa)^2A + 4(1-9\kappa^2)h_\sigma^2 + 3(1-\kappa)h_\sigma^4}{16h_\sigma^4(1+\kappa)},$$

$$\mu_1 = \frac{2\kappa^2+\kappa+8}{h_\sigma^2(1-2\kappa)}, \quad \mu_2 = \frac{3(4\kappa^4+4\kappa^3-9\kappa^2+\kappa-8)}{h_\sigma^2(1+\kappa)(1-2\kappa)^2}, \quad \mu_3 = \frac{(2\kappa^2+\kappa+8)(1-\kappa)}{2h_\sigma^2(1+\kappa)(1-2\kappa)},$$

where

$$A = h_k + uh_\sigma, \quad B = h_k^2 + 2uh_kh_\sigma + (u^2-3\kappa)h_\sigma^2, \quad h_k = \frac{\partial h}{\partial k}, \quad h_\sigma = \frac{\partial h}{\partial \sigma}.$$

References

[1] T. B. Benjamin and J. E. Feir, "The disintegration of wave trains on deep water Part 1. Theory", *J. Fluid Mech.* **27** (1967) 417–430; doi:10.1017/S002211206700045X.

[2] C. Brantenberg and I. Brevik, "Higher order water waves in currents of uniform vorticity, in the presence of surface tension", *Phys. Scr.* **47** (1993) 383–393; doi:10.1088/0031-8949/47/3/008.

[3] F. P. Bretherton and C. J. R. Garrett, "Wavetrains in inhomogeneous moving media", *Proc. Roy. Soc. Lond. Ser. A* **302** (1968) 529–554; doi:10.1098/rspa.1968.0034.

[4] U. Brinch-Nielsen and I. G. Jonsson, "Fourth order evolution equations and stability analysis for stokes waves on arbitrary water depth", *Wave Motion* **8** (1986) 455–472; doi:10.1016/0165-2125(86)90030-2.

[5] B. Chen and P. G. Saffman, "Three-dimensional stability and bifurcation of capillary and gravity waves on deep water", *Stud. Appl. Math.* **72** (1985) 125–147; doi:10.1002/sapm1985722125.

[6] S. Debsarma and K. P. Das, "Fourth order nonlinear evolution equations for gravity-capillary waves in the presence of a thin thermocline in deep water", *ANZIAM J.* **43** (2002) 513–524; doi:10.1017/S1446181100012116.

[7] A. K. Dhar and K. P. Das, "A fourth-order evolution equation for deep water surface gravity waves in the presence of wind blowing over water", *Phys. Fluids A* **2** (1990) 778–783; doi:10.1063/1.857731.

[8] A. K. Dhar and K. P. Das, "Stability analysis from fourth order evolution equation for small but finite amplitude interfacial waves in the presence of a basic current shear", *ANZIAM J.* **35** (1994) 348–365; doi:10.1017/S0334270000009346.

https://doi.org/10.1017/S1446181123000020 Published online by Cambridge University Press

[9] V. D. Djordjevic and L. G. Redekopp, "On two-dimensional packets of capillary-gravity waves", *J. Fluid Mech.* **79** (1977) 703–714; doi:10.1017/S0022112077000408.
[10] K. B. Dysthe, "Note on a modification to the nonlinear Schrödinger equation for application to deep water waves", *Proc. Roy. Soc. Lond. Ser. A* **369** (1979) 105–114; doi:10.1098/rspa.1979.0154.
[11] M. Gerber, "The Benjamin–Feir instability of a deep-water Stokes wavepacket in the presence of a non-uniform medium", *J. Fluid Mech.* **176** (1987) 311–332; doi:10.1017/S0022112087000697.
[12] R. Grimshaw and D. Pullin, "Stability of finite-amplitude interfacial waves. Part 1. Modulational instability for small-amplitude waves", *J. Fluid Mech.* **160** (1985) 297–315; doi:10.1017/S0022112085003494.
[13] K. B. Hjelmervik and K. Trulsen, "Freak wave statistics on collinear currents", *J. Fluid Mech.* **637** (2009) 267–284; doi:10.1017/S0022112009990607.
[14] S. J. Hogan, "The fourth-order evolution equation for deep-water gravity-capillary waves", *Proc. Roy. Soc. Lond. Ser. A* **402** (1985) 359–372; doi:10.1098/rspa.1985.0122.
[15] I. Kantardgi, "Effect of depth current profile on wave parameters", *Coast. Eng.* **26** (1995) 195–206; doi:10.1016/0378-3839(95)00021-6.
[16] T. Kawahara, "Nonlinear self-modulation of capillary-gravity waves on liquid layer", *J. Phys. Soc. Japan* **38** (1975) 265–270; doi:10.1143/JPSJ.38.265.
[17] B. Liao, G. Dong, Y. Ma and J. L. Gao, "Linear-shear-current modified Schrödinger equation for gravity waves in finite water depth", *Phys. Rev. E* **96** (2017) 043111; doi:10.1103/PhysRevE.96.043111.
[18] M. S. Longuet-Higgins, "The instabilities of gravity waves of finite amplitude in deep water II. Subharmonics", *Proc. Roy. Soc. Lond. Ser. A* **360** (1978) 489–505; https://royalsocietypublishing.org/doi/epdf/10.1098/rspa.1978.0081.
[19] M. S. Longuet-Higgins and R. W. Stewart, "The changes in amplitude of short gravity waves on steady non-uniform currents", *J. Fluid Mech.* **10** (1961) 529–549; doi:10.1017/S0022112061000342.
[20] J. W. McLean, "Instabilities of finite-amplitude water waves", *J. Fluid Mech.* **114** (1982) 315–330; doi:10.1017/S0022112082000172.
[21] J. W. McLean, Y. C. Ma, D. U. Martin, P. G. Saffman and H. C. Yuen, "Three-dimensional instability of finite-amplitude water waves", *Phys. Rev. Lett.* **46** (1981) 817–820; doi:10.1103/PhysRevLett.46.817.
[22] M. Onorato, D. Proment and A. Toffoli, "Triggering rogue waves in opposing currents", *Phys. Rev. Lett.* **107** (2011) 184502; doi:10.1103/PhysRevLett.107.184502.
[23] O. M. Phillips, "On the dynamics of unsteady gravity waves of finite amplitude Part 1. The elementary interactions", *J. Fluid Mech.* **9** (1960) 193–217; doi:10.1017/S0022112060001043.
[24] M. Stiassnie and L. Shemer, "On modifications of the Zakharov equation for surface gravity waves", *J. Fluid Mech.* **143** (1984) 47–67; doi:10.1017/S0022112084001257.
[25] J. R. Stocker and D. H. Peregrine, "The current-modified nonlinear Schrödinger equation", *J. Fluid Mech.* **399** (1999) 335–353; doi:10.1017/S0022112099006618.
[26] R. Tiron and W. Choi, "Linear stability of finite-amplitude capillary waves on water of infinite depth", *J. Fluid Mech.* **696** (2012) 402–422; doi:10.1017/jfm.2012.56.
[27] A. Toffoli, T. Waseda, H. Houtani, L. Cavaleri, D. Greaves and M. Onorato, "Rogue waves in opposing currents: an experimental study on deterministic and stochastic wave trains", *J. Fluid Mech.* **769** (2015) 277–297; doi:10.1017/jfm.2015.132.
[28] A. Toffoli, T. Waseda, H. Houtani, T. Kinoshita, K. Collins, D. Proment and M. Onorato, "Excitation of rogue waves in a variable medium: an experimental study on the interaction of water waves and currents", *Phys. Rev. E* **87** (2013) 051201; doi:10.1103/PhysRevE.87.051201.
[29] K. Trulsen and K. B. Dysthe, "A modified nonlinear Schrödinger equation for broader bandwidth gravity waves on deep water", *Wave Motion* **24** (1996) 281–289; doi:10.1016/S0165-2125(96)00020-0.
[30] F. M. Turpin, C. Benmoussa and C. C. Mei, "Effects of slowly varying depth and current on the evolution of a Stokes wavepacket", *J. Fluid Mech.* **132** (1983) 1–23; doi:10.1017/S0022112083001445.
[31] J. R. Wilton, "On ripples", *Phil. Mag. Series* **29** (1915) 688–700; doi:10.1080/14786440508635350.

[32] V. E. Zakharov, "Stability of periodic waves of finite amplitude on the surface of a deep fluid", *J. Appl. Mech. Tech. Phys.* **9** (1968) 190–194; doi:10.1007/bf00913182.

[33] J. Zhang and W. K. Melville, "On the stability of weakly-nonlinear gravity-capillary waves", *Wave Motion* **8** (1986) 439–454; doi:10.1016/0165-2125(86)90029-6.